THE JOURNAL OF BIOLOGICAL CHEMISTRY VOL. 287, NO. 23, pp. 19585–19598, June 1, 2012

Signal-dependent Slow Leukocyte Rolling Does Not Require Cytoskeletal Anchorage of P-selectin Glycoprotein Ligand-1 (PSGL-1) or Integrin $\alpha_L\beta_2$*[S]

Received for publication, March 12, 2012, and in revised form, April 10, 2012 Published, JBC Papers in Press, April 16, 2012, DOI 10.1074/jbc.M112.361519

Bojing Shao[‡], Tadayuki Yago[‡], Phillip A. Coghill[§¶], Arkadiusz G. Klopocki[‡], Padmaja Mehta-D'souza[‡], David W. Schmidtke[§¶], William Rodgers[‡‖], and Rodger P. McEver[‡ ‡‡1]**

*From the [‡]Cardiovascular Biology Research Program, Oklahoma Medical Research Foundation, Oklahoma City, Oklahoma 73104, the Departments of [‡‡]Biochemistry and Molecular Biology, [‖]Pathology, and **Microbiology and Immunology, University of Oklahoma Health Sciences Center, Oklahoma City, Oklahoma 73104, and the [§]University of Oklahoma Bioengineering Center and [¶]School of Chemical, Biological, and Materials Engineering, University of Oklahoma, Norman, Oklahoma 73109*

Background: The cytoskeleton contributes to receptor-initiated signaling and has been linked to force-regulated integrin activation.
Results: Disrupting cytoskeletal interactions of PSGL-1 or $\alpha_L\beta_2$ does not impair slow rolling of leukocytes on P-selectin and ICAM-1.
Conclusion: The cytoskeleton is not required for PSGL-1-initiated signals to extend $\alpha_L\beta_2$.
Significance: Signals can "prime" integrins without the cytoskeleton.

In inflamed venules, neutrophils roll on P- or E-selectin, engage P-selectin glycoprotein ligand-1 (PSGL-1), and signal extension of integrin $\alpha_L\beta_2$ in a low affinity state to slow rolling on intercellular adhesion molecule-1 (ICAM-1). Cytoskeleton-dependent receptor clustering often triggers signaling, and it has been hypothesized that the cytoplasmic domain links PSGL-1 to the cytoskeleton. Chemokines cause rolling neutrophils to fully activate $\alpha_L\beta_2$, leading to arrest on ICAM-1. Cytoskeletal anchorage of $\alpha_L\beta_2$ has been linked to chemokine-triggered extension and force-regulated conversion to the high affinity state. We asked whether PSGL-1 must interact with the cytoskeleton to initiate signaling and whether $\alpha_L\beta_2$ must interact with the cytoskeleton to extend. Fluorescence recovery after photobleaching of transfected cells documented cytoskeletal restraint of PSGL-1. The lateral mobility of PSGL-1 similarly increased by depolymerizing actin filaments with latrunculin B or by mutating the cytoplasmic tail to impair binding to the cytoskeleton. Converting dimeric PSGL-1 to a monomer by replacing its transmembrane domain did not alter its mobility. By transducing retroviruses expressing WT or mutant PSGL-1 into bone marrow-derived macrophages from PSGL-1-deficient mice, we show that PSGL-1 required neither dimerization nor cytoskeletal anchorage to signal β_2 integrin-dependent slow rolling on P-selectin and ICAM-1. Depolymerizing actin filaments or decreasing actomyosin tension in neutrophils did not impair PSGL-1- or chemokine-mediated integrin extension. Unlike chemokines, PSGL-1 did not signal cytoskeleton-dependent swing out of the β_2-hybrid domain associated with the high affinity state. The cytoskeletal independence of PSGL-1-initiated, $\alpha_L\beta_2$-mediated slow rolling differs markedly from the cytoskeletal dependence of chemokine-initiated, $\alpha_L\beta_2$-mediated arrest.

During inflammation, flowing leukocytes roll on venular surfaces, arrest, spread, crawl to endothelial junctions, and migrate into extravascular tissues (1). Selectin-ligand interactions initiate rolling, whereas integrin-ligand interactions mediate arrest and crawling (1–3). As neutrophils roll on P- or E-selectin expressed on activated endothelial cells, they transduce signals that partially activate integrin $\alpha_L\beta_2$, which binds reversibly to intercellular adhesion molecule-1 (ICAM-1)[2] to decrease rolling velocities (4, 5). Slow rolling facilitates neutrophil interactions with endothelial cell-bound chemokines that fully activate integrins, leading to arrest (6). Cooperative integrin activation by selectins and chemokines maximizes neutrophil recruitment into inflamed tissues (4).

To trigger slow rolling on ICAM-1, neutrophils rolling on P-selectin engage P-selectin glycoprotein ligand-1 (PSGL-1) (5), whereas neutrophils rolling on E-selectin engage PSGL-1 or CD44 (4, 7). The earliest identified signaling event is activation of the Src family kinases (SFKs) Fgr, Hck, and Lyn (7, 8). The activated SFKs phosphorylate the immunoreceptor tyrosine-based activation motifs on the adaptors DAP12 and Fc receptor γ (8). Spleen tyrosine kinase (Syk) docks to these motifs and is activated by SFKs. Activated Syk propagates serial activation of downstream mediators (7, 9, 10) that extend the ectodomain of

* This work was supported, in whole or in part, by National Institutes of Health Grants HL034363 and HL085607. This work was also supported by Grant HR06-102 from the Oklahoma Center for the Advancement of Science and Technology.
[S] This article contains supplemental Figs. 1–4 and Table 1.
[1] To whom correspondence should be addressed: Cardiovascular Biology Research Program, Oklahoma Medical Research Foundation, 825 N.E. 13th St., Oklahoma City, OK 73104. Tel.: 405-271-6480; Fax: 405-271-3137; E-mail: rodger-mcever@omrf.org.

[2] The abbreviations used are: ICAM-1, intercellular adhesion molecule-1; BMDM, bone marrow-derived macrophage; ERM, ezrin/radixin/moesin; FRAP, fluorescence recovery after photobleaching; SFK, Src family kinase; Syk, spleen tyrosine kinase; BisTris, 2-[bis(2-hydroxyethyl)amino]-2-(hydroxymethyl)propane-1,3-diol; PE, phycoerythrin; TMD, transmembrane domain; GpA, glycophorin A.

integrin $\alpha_L\beta_2$ but do not convert the ligand-binding site to its high affinity conformation (11).

The critical proximal events that enable PSGL-1 or CD44 to activate SFKs as neutrophils roll on P- or E-selectin are unknown. In particular, the role of the cytoskeleton in signaling has not been examined. Both PSGL-1 and CD44 are enriched in cholesterol-enriched membrane rafts (5, 7, 12). Sequestering cholesterol blocks selectin-mediated activation of SFKs and integrin-dependent slow rolling (7). In knock-in mice, PSGL-1 lacking its cytoplasmic domain mediates neutrophil rolling on P- or E-selectin but does not activate SFKs or trigger slow rolling on ICAM-1 (5, 7). *In vitro*, the PSGL-1 cytoplasmic domain binds to ezrin/radixin/moesin (ERM) proteins (5, 13, 14). ERM proteins link the cytoplasmic tails of some membrane proteins to actin filaments, and they influence the architecture of microvilli or filopodia (15). The actin cytoskeleton regulates formation of lipid rafts (16, 17) and clustering of plasma membrane proteins in both cholesterol-rich and cholesterol-poor domains (18). Cytoskeleton-directed clustering of receptors is a major mechanism to propagate signals (19, 20). Thus, neutrophils rolling on P- or E-selectin might exploit cytoskeletal anchorage of PSGL-1 to cluster small membrane domains into larger domains, increasing the local concentrations of SFKs and other mediators to initiate signaling. Anchorage of PSGL-1 might be direct or indirect. PSGL-1 lacking its cytoplasmic domain still targets to microvilli of resting neutrophils and moves to the uropods of chemokine-stimulated polarized neutrophils (5). Nevertheless, cytoplasmic domain binding to ERMs or other adaptors could anchor PSGL-1 to the cytoskeleton to facilitate signaling. PSGL-1 dimerizes through cooperative interactions of its transmembrane and cytoplasmic domains (21, 22), which might enhance interactions with ERM proteins or other adaptors. Dimerization provides a structural basis for some membrane proteins to form microclusters and to activate SFKs associated with noncatalytic receptors (23, 24).

It is also unknown whether the cytoskeleton regulates the distal events of integrin activation that slow neutrophil rolling. Integrin activation requires that talin bind to the β tail, disrupting interactions with the α tail (25). This causes the α and β legs to separate and the bent α and β ectodomains to extend the headpiece that includes the ligand-binding site. The talin head domain binds to integrin β tails, whereas the rod domain binds to actin (25). Binding of the isolated head domain to the β tail is sufficient to activate integrin $\alpha_{IIb}\beta_3$ in membrane nanodiscs (26). In cells, kindlins must also bind to β tails to fully activate integrins (25). Furthermore, force influences the conformations and therefore the functions of integrins (27–30). Force applied by flow promotes $\alpha_L\beta_2$-dependent arrest of chemokine-stimulated lymphocytes on immobilized ICAM-1 or on immobilized anti-$\alpha_L\beta_2$ mAbs that report ectodomain extension (31). Disruption of the actin cytoskeleton prevents lymphocyte arrest. It was proposed that chemokine stimulation transiently induces the extended conformation of $\alpha_L\beta_2$. Force applied to $\alpha_L\beta_2$ bound to immobilized ligand induces and/or stabilizes the high affinity conformation of the extended integrin (31). Transition to the high affinity state involves swing out of the hybrid domain from the β_2 I domain, triggering serial conformational changes in the β_2 I domain and α_L I domain (32). It was proposed that both extension and stabilization of the high affinity state require prior anchorage of the integrin to the cytoskeleton (31). Recent data indicate that cells activated by chemokines or other agonists only modestly increase $\alpha_L\beta_2$ affinity for ICAM-1 (33). Binding of "primed" $\alpha_L\beta_2$ to immobilized, but not fluid-phase, ICAM-1 triggers energy-dependent conversion of $\alpha_L\beta_2$ to its high affinity state (33). These data support a model in which the cytoskeleton exerts lateral force on talin and/or kindlins to fully separate the integrin α and β tails and convert the extended ectodomain to the high affinity state, if the primed integrin binds to immobilized ligand (34). Signaling through PSGL-1 also primes $\alpha_L\beta_2$. However, PSGL-1-primed $\alpha_L\beta_2$ bound to immobilized ICAM-1 under flow does not transition to a high affinity state (35). Whether PSGL-1-primed $\alpha_L\beta_2$ requires cytoskeletal anchorage to rapidly extend and mediate slow rolling has not been explored. If $\alpha_L\beta_2$ does not attach to the cytoskeleton, forces are likely to be applied axially but not laterally during rolling on ICAM-1.

Here, we tested these concepts by manipulating cytoskeletal anchorage or dimerization of PSGL-1 and by depolymerizing actin filaments or decreasing actomyosin tension. Remarkably, PSGL-1 did not have to dimerize or attach to the cytoskeleton to trigger $\alpha_L\beta_2$-mediated slow rolling on P-selectin and ICAM-1. Indeed, rapid extension of $\alpha_L\beta_2$ in the low affinity state by PSGL-1 signals and unexpectedly by initial chemokine signals did not need actin filaments or actomyosin tension. Additional chemokine signals, however, required actin filaments and actomyosin tension to arrest rolling cells on ICAM-1 or on a mAb to an $\alpha_L\beta_2$ conformation associated with high affinity for ligand.

EXPERIMENTAL PROCEDURES

Reagents—Rat anti-murine PSGL-1 monoclonal antibody (mAb, clone 4RA10), phycoerythrin (PE)-labeled rat anti-murine PSGL-1 mAb (clone 2PH1), and hamster anti-murine CD54 mAb (clone 3E2) were from Pharmingen. FITC-labeled rat anti-murine CD11a (α_L integrin subunit) mAb (clone M17/4), rat anti-murine CD11a mAb (clone M17/4), FITC-labeled rat anti-murine CD11b mAb (clone M1/70), rat anti-murine CD11b mAb (clone M1/70), FITC-labeled rat anti-murine F4/80 mAb (clone C1:A3-1), and FITC-labeled rat anti-murine Ly6G/C mAb (clone RB6-8C5) were from BioLegend Inc. (San Diego). Murine anti-human PSGL-1 mAb PL1 was generated as described previously (36). Murine anti-human CD18 (β_2 integrin subunit) (clone MEM148) was from Abcam (San Francisco). Murine anti-human β_2 integrin subunit (clone IB4) was from American Type Culture Collection (Manassas, VA). Murine anti-human β2 integrin subunit (clone KIM127) was a gift from Nancy Hogg (London Research Institute, London, UK). FITC-labeled goat anti-mouse IgG, purified goat anti-human IgM, 10% *n*-dodecyl-β-D-maltoside, and Native-PAGE BisTris gel, pZeoSV2(−) vector, and calcium phosphate transfection kit were from Invitrogen. Murine anti-moesin mAb (clone 38/87) and horseradish peroxidase-conjugated goat anti-murine IgG were from Thermo Scientific (Fremont, CA). Horseradish peroxidase-conjugated goat anti-rat IgG was from Cell Signaling Technology (Danvers, MA). Recombinant murine ICAM-1 Fc chimera, recombinant murine CCL2, recombinant murine

CXCL1, and recombinant human IL-8 were from R&D Systems (Minneapolis, MN). Piceatannol, filipin III, methyl-β-cyclodextrin, α-cyclodextrin, latrunculin B, blebbistatin, and Polybrene were from Sigma. 4-Amino-5-(4-chlorophenyl)-7-(*t*-butyl)pyrazolo[3,4-*d*]pyrimidine (PP2) and 4-amino-7-phenylpyrazolo[lsqb]3,4-*d*]pyrimidine (PP3) were from Calbiochem). Murine P-selectin-IgM chimeras were described previously (37). F-actin visualization biochem kit was from Cytoskeleton, Inc. (Denver, CO). All restriction endonucleases and T4 DNA ligase were from New England Biolabs (Ipswich, MA). *Pfu*Turbo DNA polymerase was from Stratagene (La Jolla, CA). pGEX-5X-3 vector was from GE Healthcare. Retroviral vector MSCV-IRES-GFP (pMiG) (38) was a gift from Jose Alberola-IIa (Oklahoma Medical Research Foundation, Oklahoma City, OK). Phoenix™ Eco cells and Pway 20 vector containing cDNA encoding yellow fluorescent protein (YFP) have been described (39). Colony-stimulating factor-1-conditioned medium (40) was a gift from Mark Coggeshall (Oklahoma Medical Research Foundation, Oklahoma City, OK).

Mice—PSGL-1$^{-/-}$ mice were generated as described previously (37). C57BL/6J (B6, CD45.2) mice were purchased from The Jackson Laboratory (Bar Harbor, ME). DAP12$^{-/-}$/FcRγ$^{-/-}$ and Hck$^{-/-}$/Fgr$^{-/-}$/Lyn$^{-/-}$ mice were gifts from Clifford Lowell (University of California, San Francisco). Btk$^{-/-}$ mice were provided by Wasif Khan (Vanderbilt University). The original references for these mice have been cited (7). All experiments were performed in compliance with protocols approved by the Institutional Animal Care and Use Committee of the Oklahoma Medical Research Foundation.

Generation of Recombinant Proteins—Recombinant proteins were generated as described previously (5) with minor modifications. Briefly, constructs encoding GST fusion proteins were generated using synthetic oligonucleotides encoding the WT or mutated murine PSGL-1 cytoplasmic domains with BamHI and EcoRI sites appended, respectively, at the 5′ and 3′ ends. Oligonucleotides were ligated into the pGEX-5×-3 vector. Constructs were confirmed by DNA sequencing. BL21 *Escherichia coli* (Stratagene) cells were transformed with vectors encoding each construct. The GST fusion proteins were purified using glutathione-Sepharose 4B resin (GE Healthcare) according to the manufacturer's instructions. GST fusion proteins attached to the resins were stored in Buffer A (10 mM Hepes buffer, pH 7.5, 150 mM KCl, 1 mM $MgCl_2$, 1 mM EGTA, 1 mM DTT, 2 μg/ml leupeptin) at 4 °C.

Pulldown Assay—Binding of moesin to GST fusion proteins was measured as described previously (5).

Generation of PSGL-1 Constructs—A full-length cDNA encoding murine PSGL-1 in the vector pZeoSV2(−) (5) was used as template for generating mutants. Residues in the juxtamembrane region of the cytoplasmic domain reported to confer binding to ERM proteins were replaced with alanines by PCR-based site-directed mutagenesis. To produce chimeras, the transmembrane domain of PSGL-1 was swapped with that of murine CD43 or glycophorin A by overlap extension PCR. To prepare constructs for retroviral transduction, cDNAs encoding WT or mutant PSGL-1 were cloned into the retroviral vector pMiG containing cDNA for GFP, with XhoI and HpaI sites at the 5′ and 3′ ends, respectively. To prepare YFP fusion proteins, all PSGL-1 constructs were subcloned into a pWay20 vector containing cDNA for monomeric YFP (41) with BamHI and SmaI sites at the 5′ and 3′ ends, respectively. All constructs were confirmed by DNA sequencing.

Transfected Cells—Transfected Chinese hamster ovary (CHO) cells stably expressing core 2 GlcNAcT-I and FucT-VII (42) were transfected with cDNAs encoding murine PSGL-1 constructs in the pZeoSV2(−) vector. Stable clones expressing PSGL-1 constructs were selected with 600 μg/ml G418, 100 μg/ml hygromycin, and 250 μg/ml Zeocin. CHO cells not expressing core 2 GlcNAcT-I and FucT-VII were transfected with cDNAs encoding YFP-fused PSGL-1 constructs in the pWay20 vector. Stable clones expressing YFP-fused PSGL-1 constructs were selected with 600 μg/ml G418. Cells expressing matched surface densities of PSGL-1 constructs or YFP fusion proteins were isolated using anti-murine PSGL-1 mAb in the cell sorting facility of the Oklahoma Medical Research Foundation.

Fluorescence Recovery after Photobleaching (FRAP)—Stable CHO cell lines expressing YFP-fused murine PSGL-1 constructs were seeded onto glass-bottomed tissue culture dishes and allowed to grow overnight. Cells were imaged on an inverted confocal laser scanning microscope equipped with a 37 °C heated stage, a ×63 objective, and a META detector (LSM 510, Zeiss, Germany). YFP fluorescence (527–580 nm) excited by the argon/krypton 514 laser light and a 458/514 nm beam splitter was detected with the META detector. After acquiring overview images of single cells, regions of interest (12 or 41 μm^2) were photobleached with 25 iterations of 75–100% maximum 514-nm laser power. Subsequently, time-lapse images were collected at 1–5% laser power until the bleached signal reached a stable level. With Zeiss imaging software, movies were generated, and fluorescence recovery over time was quantified as described previously (43). Briefly, FRAP curves from five independent trials with 3–5 measurements per trial were fitted to a function for monoexponential recovery of fluorescence using Igor Pro software (Version 5.04B, WaveMetrics Inc., Portland, OR). This fitting was used to determine F_{max}, which represents the fraction of recovery at infinite time and therefore the mobile fraction of the molecule in the bleached region, or, inversely, its immobile fraction, and τ, which is the time constant for recovery and is inversely proportional to the diffusion coefficient. Means ± S.E. for τ and F_{max} derived by curve fitting are reported in Table 1 and supplemental Table 1.

Retroviral Infections—Phoenix™ Eco cells were transfected with 20 μg of murine PSGL-1 constructs in the pMiG vector by calcium phosphate precipitation. After 12 h, the culture medium was replaced, and the cells were cultured for an additional 48 h. Virus particles released into the medium were concentrated by centrifugation at 19,500 × *g* for 2 h. Bone marrow-derived macrophages (BMDMs) from WT or PSGL-1$^{-/-}$ mice were generated as described previously (40). The concentrated virus was added to BMDMs from PSGL-1$^{-/-}$ mice in the presence of 20 μg/ml Polybrene for 12 h. The medium was replaced, and the cells were cultured for an additional 4 days.

Immunofluorescence—Murine bone marrow leukocytes, BMDMs, or human neutrophils treated with DMSO or latrun-

culin B were fixed and permeabilized with the buffer in the F-actin visualization biochem kit. The cells were stained with rhodamine-phalloidin following the manufacturer's instruction and allowed to adhere to polylysine-coated coverslips. Immunofluorescence was detected with a confocal laser scanning microscope equipped with an argon/krypton laser light (LSM 510, Zeiss, Germany).

SFK, Syk, and p38 Phosphorylation—The activation of SFKs, Syk, and p38 in bone marrow leukocytes or BMDMs plated on P-selectin was measured as described previously (7).

Blue Native-PAGE—Blue native-PAGE was performed according to the protocol from the manufacturer (Invitrogen). Briefly, cells were lysed with 1% *n*-dodecyl-β-D-maltoside on ice, and the lysates were centrifuged at 15,000 × *g* for 30 min at 4 °C. The supernatant was mixed with Native-PAGE sample buffer. After electrophoresis, resolved proteins were transferred to polyvinylidene difluoride membranes and blotted with anti-murine PSGL-1 mAb 4RA10.

Western Blots—Western blots were performed as described previously (37, 42).

Flow Cytometry—Flow cytometry was performed as described previously (37, 42). In some experiments, human neutrophils were preincubated with latrunculin B (1 μM) and/or blebbistatin (10 μM) or with control DMSO for 30 min and then stimulated with 0.5 nM IL-8 for 5 min. The cells were then incubated with 20 μg/ml mAb IB4, KIM127, or MEM148 and then with PE-conjugated anti-mouse IgG. In other experiments, human neutrophils pretreated with DMSO or latrunculin B were incubated with 50 μg/ml of human platelet-derived P-selectin (44) for 30 min and then stained with IB4, KIM127, or MEM148.

Flow Chamber Assay—Adhesion of transduced BMDMs under flow was measured with microfluidic flow chambers that were fabricated from polydimethylsiloxane by photolithography procedures described previously (45, 46). The microfluidic channel had dimensions of 1 mm in width and 100 μm in height, and the microfluidic channel was sealed to a glass coverslip by pretreatment of the polydimethylsiloxane with a high frequency generator. To prepare the chamber, a mAb recognizing human IgM (10 μg/ml) was absorbed onto the glass floor of the microfluidic chamber at room temperature for 1 h. In some experiments, ICAM-1-Fc chimera (20 μg/ml) with or without CCL2 (10 μg/ml) was also adsorbed. After blocking the chambers with 2% human serum albumin for 2 h, murine P-selectin-IgM was captured to the immobilized anti-human IgM mAb.

To study human neutrophils, murine bone marrow leukocytes, and nontransduced BMDMs, we used a 35-mm culture dish as described previously (7). For murine bone marrow leukocytes or BMDMs, ICAM-1-Fc chimera (20 μg/ml) was adsorbed with or without CXCL1 or CCL2 (10 μg/ml), respectively. Murine P-selectin-IgM was captured to immobilized anti-human IgM mAb. For human neutrophils, ICAM-1, KIM127, or MEM148 was coimmobilized with human P-selectin with or without coimmobilized IL-8.

BMDMs, murine bone marrow leukocytes, or human neutrophils (10^6/ml in Hanks' balanced salt solution with 0.5% human serum albumin) were perfused over the substrates in chambers at a wall shear stress of 1 dyn/cm^2. In some experiments, chambers were pretreated with anti-ICAM-1 mAb (20 μg/ml) or cells were pretreated with 20 μg/ml anti-$\alpha_L\beta_2$ mAb, anti-$\alpha_M\beta_2$ mAb, or isotype-matched control mAb. In other experiments, cells were preincubated with the Syk inhibitor piceatannol (20 μM), the SFK inhibitor PP2, or its inactive analog PP3 (20 μM), the p38 inhibitor SB203580 (50 μM), latrunculin B (1 μM), blebbistatin (10 μM), or an equal volume of DMSO as vehicle control. For some studies, membrane lipid rafts were disrupted before perfusing cells over P-selectin (7). After 5 min, velocities of rolling cells were measured over a 5-s interval using a video microscope coupled to a digital analysis system on a Silicon Graphics workstation.

Statistics—Data are expressed as mean ± S.E. Comparisons used the Student's *t* test.

RESULTS

Juxtamembrane Residues in the Cytoplasmic Domain of PSGL-1 Restrain Its Membrane Mobility—ERM proteins bind to the juxtamembrane regions of the cytoplasmic domains of some membrane proteins. Early studies suggested that ERM proteins rely on electrostatic interactions to bind to clustered basic residues in the cytoplasmic domains (47). However, crystal structures revealed that ERM proteins also dock to other juxtamembrane residues that strengthen binding (48). We expressed GST proteins fused to the murine WT PSGL-1 cytoplasmic domain or to two mutants that substituted alanines for different groups of juxtamembrane residues (Fig. 1*A*). One mutant, termed SRKS, was based on a report that replacing the targeted residues decreased binding of the PSGL-1 cytoplasmic domain to moesin (13). The other mutant, termed MYVR, was based on a crystal structure in which radixin contacted each of the targeted residues in the PSGL-1 cytoplasmic domain (48). We incubated GST alone or each GST fusion protein with recombinant moesin, recovered bound complexes on glutathione resin, and analyzed bound proteins by SDS-PAGE and Western blotting with anti-moesin antibody. The WT and MYVR PSGL-1 constructs pulled down moesin, whereas GST alone or the SRKS PSGL-1 construct did not (Fig. 1*B*). These results suggest that the SRKS residues in the PSGL-1 tail dominate binding to moesin in this assay but do not exclude a role for the MYVR residues in intact cells.

Binding of the cytoplasmic domain to ERM proteins or other adaptors could anchor PSGL-1 to the cytoskeleton and restrict its mobility in the plasma membrane. To address this possibility, we prepared full-length constructs of WT or mutant PSGL-1, each fused to monomeric YFP (41) at the C-terminal end of the cytoplasmic domain (Fig. 1*C*). Each construct was stably expressed in transfected CHO cells. We used FRAP to measure mobility of the fluorescent construct in a region of the plasma membrane (41 μm^2) that was photobleached by a brief laser pulse. Recovery of fluorescence by diffusion of PSGL-1-YFP constructs into the bleached region was measured by acquiring serial images. The initial photobleach destroys the fluorescence in the mobile and immobile pools of the PSGL-1-YFP construct, and the maximal fluorescence recovery (F_{max}) indicates the mobile fraction. F_{max} reflects the fraction of PSGL-1-YFP proteins that dynamically bind to and unbind from less mobile structures such as the cytoskeleton. The F_{max}

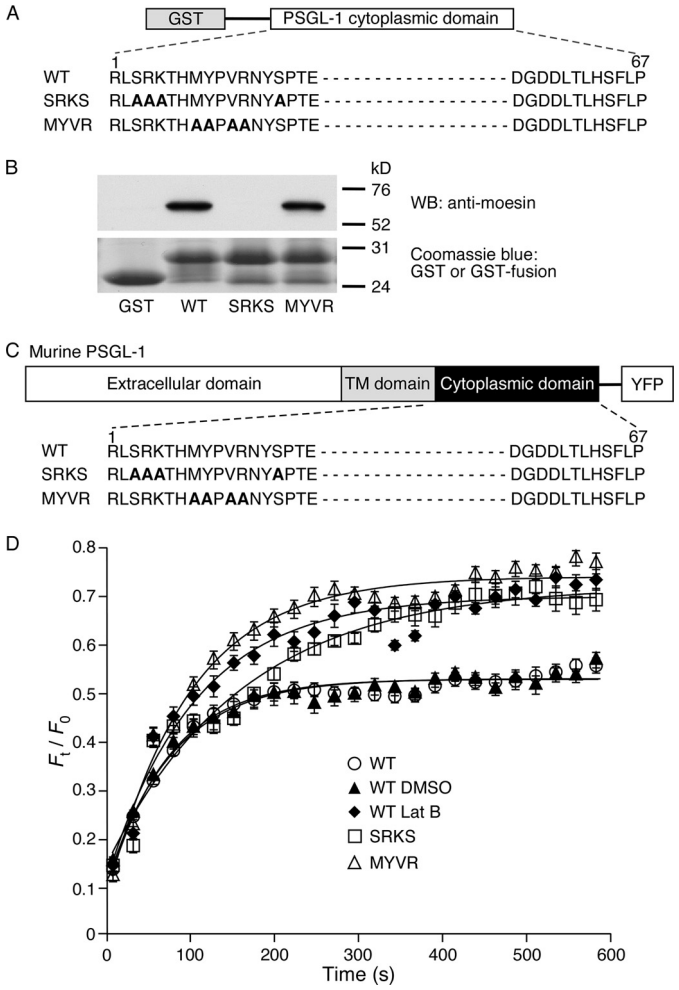

FIGURE 1. **Juxtamembrane residues in the cytoplasmic domain of PSGL-1 restrain its membrane mobility.** *A,* schematic diagram of GST or GST fused to the entire cytoplasmic domain of murine WT PSGL-1 or to the cytoplasmic domain in which two groups of residues (SRKS or MYVR) implicated in binding to ERM proteins were substituted with alanines. *B,* recombinant moesin was incubated with GST or GST fusion proteins. Precipitated protein was eluted and probed by Western blot (*WB*) with anti-moesin antibody under reducing conditions. Equivalent loading was confirmed by Coomassie Blue staining of GST or GST fusion proteins. Results are representative of three experiments. Molecular weight standards are indicated. *C,* schematic diagram of YFP fusion proteins. YFP was fused to the C terminus of WT murine PSGL-1 or PSGL-1 in which two groups of cytoplasmic domain residues (SRKS or MYVR) implicated in binding to ERM proteins were substituted with alanines. *D,* plot of normalized fluorescence intensity values *versus* time after photobleaching a small area of peripheral membrane (41 μm^2) of transfected CHO cells expressing the indicated PSGL-1-YFP construct in the presence or absence of DMSO or latrunculin B (*Lat B*). FRAP curves from five independent trials with 3–5 measurements per trial were fitted to a function for monoexponential recovery of fluorescence (see "Experimental Procedures") to derive τ and F_{max} as reported in Table 1. The data represent the mean ± S.E.

of WT PSGL-1-YFP was the same in untreated cells or in cells treated with the vehicle control DMSO (Fig. 1*D*). In contrast, the F_{max} of WT PSGL-1-YFP increased in cells treated with latrunculin B, which depolymerizes actin by sequestering G actin and preventing F-actin assembly (49). This result suggests that the mobile fraction of WT PSGL-1 is restricted by interactions with the actin-based cytoskeleton. The F_{max} of both PSGL-1-YFP mutants was higher in untreated or DMSO-treated cells and matched the F_{max} of WT PSGL-1-YFP in latrunculin B-treated cells (Fig. 1*D* and Table 1). Similar results

TABLE 1

Kinetic analysis of FRAP in transfected CHO cells expressing PSGL-1-YFP constructs

FRAP curves (see Figs. 1 and 2) from five independent trials with 3–5 measurements per trial were fitted to a function for monoexponential recovery of fluorescence (see "Experimental Procedures") to derive τ and F_{max}. The data represent the mean ± S.E.

PSGL-1/cell treatment	τ[a]	F_{max}[b]
	s	
WT	207 ± 19	0.6 ± 0.1
WT/DMSO	212 ± 20	0.6 ± 0.1
WT/latrunculin B	93 ± 13[c]	0.7 ± 0.1[c]
SRKS	202 ± 20	0.7 ± 0.1[c]
MYVR	84 ± 13[c]	0.8 ± 0.1[c]
CD43 TMD	226 ± 17	0.5 ± 0.1
GpA TMD	213 ± 16	0.6 ± 0.1

[a] τ indicates the time constant for fluorescence recovery.
[b] F_{max} indicates the maximum fluorescence recovery.
[c] $p < 0.01$ compared with WT.

were observed in a second set of experiments that reduced the area of plasma membrane that was photobleached (12 μm^2) (supplemental Fig. 1 and Table 1). In those experiments, treating the cells with latrunculin B did not further increase the F_{max} values of the mutants (supplemental Fig. 1 and Table 1). This suggests that each group of mutations impaired interactions of PSGL-1 with the cytoskeleton, increasing the mobile fraction.

The time constant of recovery (τ) is inversely proportional to the rate of diffusion of the mobile protein, and thus reports the relative molecular mobility of labeled protein in the plasma membrane. τ decreased when the photobleached area decreased (compare Table 1 and supplemental Table 1), indicating that recovery was due to diffusion in the membrane rather than to nondiffusive processes such as trafficking from a separate compartment (50). The τ of MYVR PSGL-1-YFP was much shorter and was similar to the τ for WT PSGL-1-YFP in latrunculin B-treated cells (Fig. 1*D* and Table 1). Treating the cells with latrunculin B did not further decrease the τ of MYVR PSGL-1-YFP (supplemental Fig. 1 and Table 1). This suggests disrupted interactions of this mutant with the cytoskeleton, causing its rate of diffusion to reach that in cells that lacked intact actin filaments. In contrast, the τ of SRKS PSGL-1-YFP was similar to that of WT PSGL-1-YFP in untreated or DMSO-treated cells (Fig. 1*D* and Table 1). Latrunculin B decreased the τ values of WT and SRKS PSGL-1-YFP to the same level (supplemental Fig. 1 and Table 1). This implies weakened but not completely disrupted interactions of SRKS PSGL-1-YFP with the cytoskeleton, increasing its mobile fraction without affecting its rate of diffusion. Collectively, these data demonstrate that the membrane mobility of PSGL-1 is restrained by interactions of its cytoplasmic domain with the actin cytoskeleton. Two distinct sets of juxtamembrane mutations in the PSGL-1 cytoplasmic domain weaken and/or disrupt these interactions.

Dimerization of PSGL-1 Does Not Restrain Its Membrane Mobility—Dimerization of membrane proteins can slow their mobilities and favor formation of microclusters (23, 51). To determine whether dimerization regulates the mobility of PSGL-1, we expressed dimeric and monomeric forms of PSGL-1-YFP (Fig. 2*A*). PSGL-1 forms dimers through noncovalent interactions of the transmembrane and cytoplasmic domains, which are stabilized by a single extracellular disulfide bond (21, 22). Mutating the extracellular cysteine and replacing the trans-

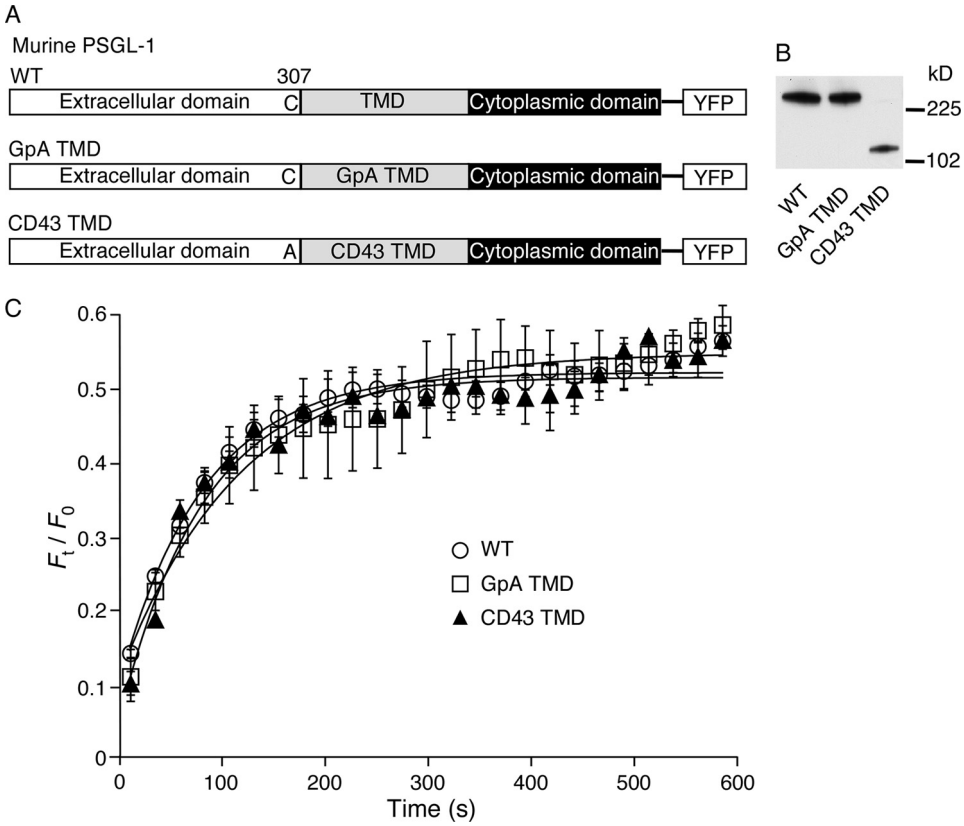

FIGURE 2. **Dimerization of PSGL-1 does not restrain its membrane mobility.** *A,* schematic diagram of YFP fusion proteins. YFP was fused to the C terminus of WT murine PSGL-1 or PSGL-1 in which the transmembrane domain (*TMD*) was substituted with that of glycophorin A (*GpA*) or CD43. The CD43 TMD construct also replaced the juxtamembrane cysteine 307 with alanine. *B,* lysates from transfected CHO cells expressing matched densities of the indicated PSGL-1 construct were resolved by native gel electrophoresis and probed by Western blot with anti-PSGL-1 mAb. Molecular weight standards are indicated. *C,* plot of normalized fluorescence intensity values *versus* time after photobleaching a small area of peripheral membrane (41 μm^2) of transfected CHO cells expressing the indicated PSGL-1-YFP construct. FRAP curves from five independent trials with 3–5 measurements per trial were fitted to a function for monoexponential recovery of fluorescence (see "Experimental Procedures") to derive τ and F_{max} as reported in Table 1. The data represent the mean ± S.E.

membrane domain with the transmembrane domain of CD43 generates a monomeric form of PSGL-1 (CD43 TMD PSGL-1) (21). Substituting the transmembrane domain of PSGL-1 with that of glycophorin A creates an alternative dimeric form of PSGL-1 (GpA TMD PSGL-1) (22). Each construct was stably expressed in transfected CHO cells. Western blots of cell lysates resolved by nondenaturing gel electrophoresis confirmed that WT PSGL-1 and GpA TMD PSGL-1 migrate as dimers, whereas CD43 TMD PSGL-1 migrates as monomers (Fig. 2*B*). FRAP measurements revealed indistinguishable F_{max} and τ values for all three PSGL-1-YFP constructs (Fig. 2*C* and Table 1). Thus, the mobilities of dimeric and monomeric PSGL-1 are similar.

Cytoskeletal Anchorage of PSGL-1 Is Not Required to Trigger β_2 Integrin-mediated Slow Rolling on P-selectin and ICAM-1—The data in Fig. 1 indicate that juxtamembrane residues in the cytoplasmic domain tether PSGL-1 to the cytoskeleton. To determine whether these interactions influence the signaling functions of PSGL-1, we used BMDMs as a model system. BMDMs are nontransformed cells of myeloid lineage that can be transduced with retroviruses expressing recombinant proteins (40). BMDMs expressed the myeloid markers Ly6G/Lys6C and the macrophage marker F4/80 (supplemental Fig. 2*A*). Neutrophils express similar levels of integrins $\alpha_L\beta_2$ and $\alpha_M\beta_2$ (52), whereas BMDMs expressed more $\alpha_M\beta_2$ than $\alpha_L\beta_2$ (supplemental Fig. 2*B*). BMDMs rolled on immobilized P-selectin and rolled more slowly on P-selectin coimmobilized with ICAM-1. The slower rolling was partially inhibited by mAb to $\alpha_L\beta_2$ or $\alpha_M\beta_2$ and was abrogated by mAb to ICAM-1 (Fig. 3*A*) or by mAbs to both $\alpha_L\beta_2$ and $\alpha_M\beta_2$ (see Fig. 6*B*). Slow rolling of BMDMs on P-selectin plus ICAM-1 was blocked by agents that disrupt lipid rafts or by the SFK inhibitor PP2, the Syk inhibitor piceatannol, or the p38 MAPK inhibitor SB202190 (Fig. 3, *B–D*). Furthermore, slow rolling was not observed in BMDMs from mice lacking the SFKs Fgr, Hck, and Lyn, lacking Bruton's tyrosine kinase, or lacking Fc receptor γ and DAP12 (Fig. 3, *C* and *E*). Like bone marrow leukocytes, BMDMs plated on immobilized P-selectin activated Syk and p38, as measured by Western blotting of cell lysates with antibodies to the phosphorylated forms of these proteins (Fig. 3*F*). Kinase activation did not occur in BMDMs plated on immobilized control protein or on P-selectin in buffer containing EDTA to inhibit Ca^{2+}-dependent interactions between P-selectin and PSGL-1. Thus, BMDMs trigger β_2 integrin-dependent slow rolling on P-selectin and ICAM-1 through a signaling cascade that is indistinguishable from that used by neutrophils. These data validate the utility of BMDMs to study PSGL-1-mediated signaling in neutrophils.

We transduced BMDMs from PSGL-$1^{-/-}$ mice with retroviruses expressing WT PSGL-1, SRKS PSGL-1, or MYVR

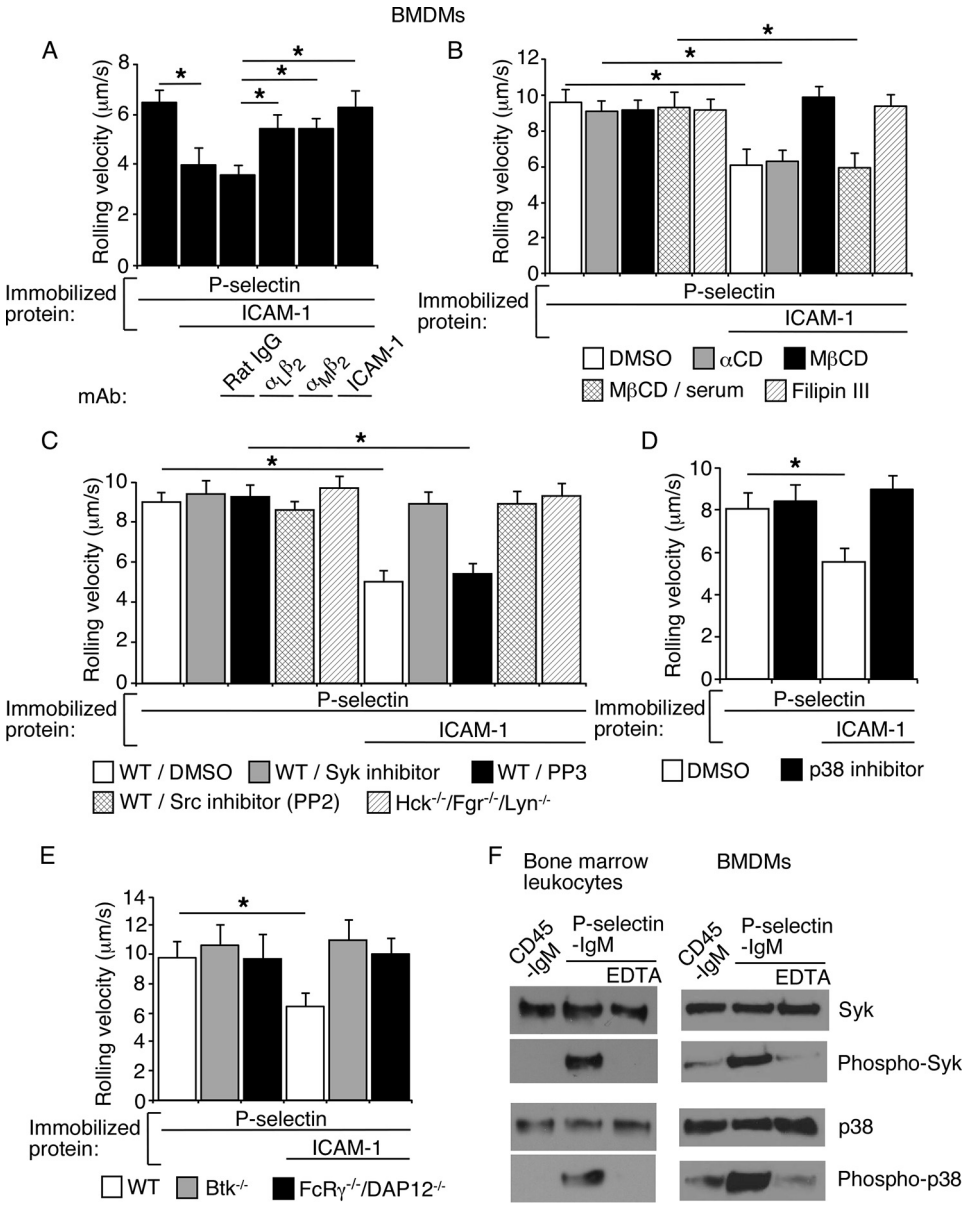

FIGURE 3. **Murine BMDMs rolling on P-selectin use the same signaling cascade as murine bone marrow leukocytes to trigger β_2 integrin-dependent slow rolling on ICAM-1.** *A,* velocities of WT BMDMs rolling on P-selectin with or without coimmobilized ICAM-1 in the presence or absence of the indicated mAb. *B,* velocities of WT BMDMs rolling on P-selectin with or without coimmobilized ICAM-1 in the presence or absence of the vehicle control DMSO, methyl-β-cyclodextrin (*MβCD*) or its inactive analog α-cyclodextrin (*αCD*), MβCD plus 15% serum (to restore membrane cholesterol), or filipin III. *C,* velocities of WT or Hck$^{-/-}$/Fgr$^{-/-}$/Lyn$^{-/-}$ BMDMs rolling on P-selectin with or without coimmobilized ICAM-1 in the presence or absence of the vehicle control DMSO, the Syk inhibitor piceatannol, the Src family kinase inhibitor PP2, or its inactive analog PP3. *D,* velocities of WT BMDMs rolling on P-selectin with or without coimmobilized ICAM-1 in the presence of the vehicle control DMSO or the p38 inhibitor SB202190. *E,* velocities of WT, Btk$^{-/-}$, or FcRγ$^{-/-}$/DAP12$^{-/-}$ BMDMs rolling on P-selectin with or without coimmobilized ICAM-1. The wall shear stress in *A–E* was 1 dyn/cm^2. The data in *A–F* represent the mean ± S.E. from at least three experiments. *, $p < 0.01$. *F,* bone marrow leukocytes or BMDMs from WT mice were rotated on immobilized P-selectin-IgM in the presence or absence of EDTA or on control CD45-IgM for 5 min. Lysates were probed by Western blotting with the indicated antibody. The data are representative of three experiments.

PSGL-1. The transduced cells were sorted to match surface expression of each recombinant PSGL-1 to approximately the same level as native PSGL-1 on BMDMs from WT mice (Fig. 4*A*). Mock-transduced PSGL-1$^{-/-}$ BMDMs did not roll on P-selectin (data not shown). Transduced PSGL-1$^{-/-}$ cells expressing each recombinant PSGL-1 rolled on P-selectin with similar mean velocity as BMDMs from WT mice expressing native PSGL-1 (Fig. 4*B*). Rolling was blocked by mAbs to P-selectin or PSGL-1 (data not shown). Like WT BMDMs expressing native PSGL-1, transduced PSGL-1$^{-/-}$ BMDMs expressing each recombinant PSGL-1 rolled significantly slower on P-selectin and ICAM-1 (Fig. 4*B*). These data demonstrate that PSGL-1 need not attach its cytoplasmic tail to the cytoskeleton to signal integrin-dependent slow rolling.

Dimerization of PSGL-1 Is Not Required to Trigger β_2 Integrin-mediated Slow Rolling on P-selectin and ICAM-1—We transduced BMDMs from PSGL-1$^{-/-}$ mice with retroviruses expressing WT PSGL-1, CD43 TMD PSGL-1, or GpA TMD PSGL-1. The transduced cells were sorted to match surface expression of each recombinant PSGL-1 to approximately the

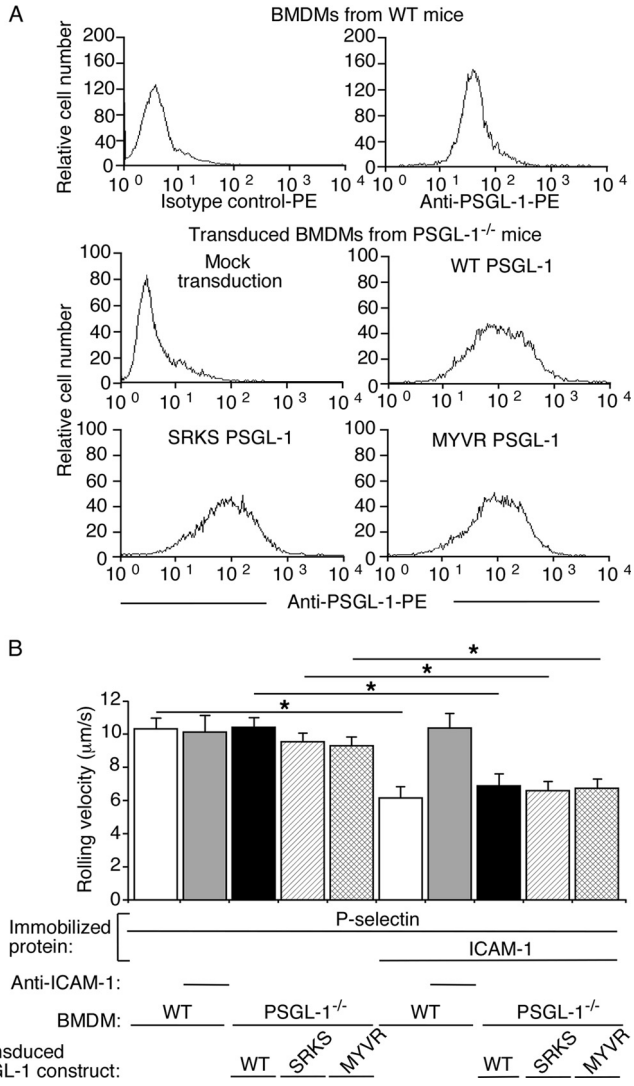

FIGURE 4. **Cytoskeletal anchorage of PSGL-1 is not required to trigger β_2 integrin-mediated slow rolling on P-selectin and ICAM-1.** *A,* flow cytometric analysis of BMDMs from WT or PSGL-1$^{-/-}$ mice incubated with PE-labeled isotype control mAb or anti-PSGL-1 mAb. BMDMs from PSGL-1$^{-/-}$ mice were mock-transduced or transduced with retroviruses expressing WT PSGL-1, SRKS PSGL-1, or MYVR PSGL-1. The data are representative of at least three experiments. *B,* velocities of WT BMDMs or of transduced PSGL-1$^{-/-}$ BMDMs expressing WT PSGL-1, SRKS PSGL-1, or MYVR PSGL-1 rolling on P-selectin with or without coimmobilized ICAM-1 in the presence or absence of blocking mAb to ICAM-1. The wall shear stress in all experiments was 1 dyn/cm^2. The data represent the mean ± S.E. from at least three experiments. *, $p < 0.01$.

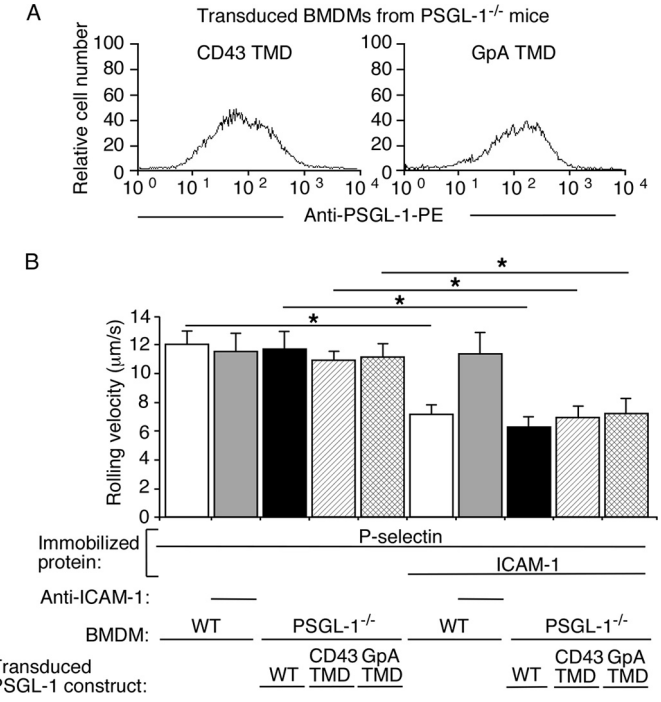

FIGURE 5. **Dimerization of PSGL-1 is not required to trigger β_2 integrin-mediated slow rolling on P-selectin and ICAM-1.** *A,* flow cytometric analysis of transduced BMDMs from PSGL-1$^{-/-}$ mice expressing the indicated PSGL-1 construct. The cells were incubated with PE-labeled anti-PSGL-1 mAb. The data are representative of at least three experiments. *B,* velocities of WT BMDMs or transduced PSGL-1$^{-/-}$ BMDMs expressing the indicated PSGL-1 construct rolling on P-selectin with or without coimmobilized ICAM-1 in the presence or absence of blocking mAb to ICAM-1. The wall shear stress in all experiments was 1 dyn/cm^2. The data represent the mean ± S.E. from at least three experiments. *, $p < 0.01$.

same level as native PSGL-1 on BMDMs from WT mice (Fig. 5*A*). Transduced cells expressing each recombinant PSGL-1 rolled on P-selectin with similar mean velocity as BMDMs expressing native PSGL-1 (Fig. 5*B*). Rolling was blocked by mAbs to P-selectin or PSGL-1 (data not shown). Furthermore, BMDMs expressing each recombinant PSGL-1 rolled significantly slower on P-selectin and ICAM-1 (Fig. 5*B*). These data demonstrate that dimerization of PSGL-1 is not required to signal integrin-dependent slow rolling.

Neutrophils or BMDMs Do Not Require an Intact Actin Cytoskeleton to Initiate Signaling and Induce β_2 Integrin-mediated Slow Rolling on P-selectin and ICAM-1—The cytoplasmic domain mutations increased the mobile fraction of PSGL-1 to that of WT PSGL-1 in transfected cells treated with latrunculin B to depolymerize actin filaments. Because BMDMs expressing the PSGL-1 mutants triggered integrin-dependent slow rolling, the cytoplasmic tail need not directly attach to the cytoskeleton to initiate signaling. However, the cells might require the actin-based cytoskeleton to assemble kinases or other mediators that cause β_2 integrins to extend to slow rolling. To test this hypothesis, we treated human neutrophils or bone marrow leukocytes or BMDMs from WT mice with vehicle control DMSO or with latrunculin B. Immunofluorescence microscopy confirmed that latrunculin B markedly decreased phalloidin staining of actin filaments along the plasma membrane (supplemental Fig. 3, *A* and *B*). Latrunculin B did not alter the surface density of PSGL-1 on murine neutrophils or BMDMs (supplemental Fig. 4). When plated on immobilized P-selectin, both DMSO- and latrunculin B-treated human neutrophils and murine bone marrow leukocytes activated SFKs, as measured by Western blotting of cell lysates with antibody to the phosphorylated forms of these proteins (Fig. 6*A*). Kinase activation did not occur in leukocytes plated on immobilized control protein or on P-selectin in buffer containing EDTA to inhibit Ca^{2+}-dependent interactions between P-selectin and PSGL-1. Over 90% of murine bone marrow leukocytes that roll on P- or E-selectin are neutrophils (5, 7). At the shear stresses tested, latrunculin B treatment did not alter the velocities of murine BMDMs or neutrophils rolling on P-selectin or on P-selectin plus ICAM-1 (Fig. 6, *B* and *C*). These results demonstrate that nei-

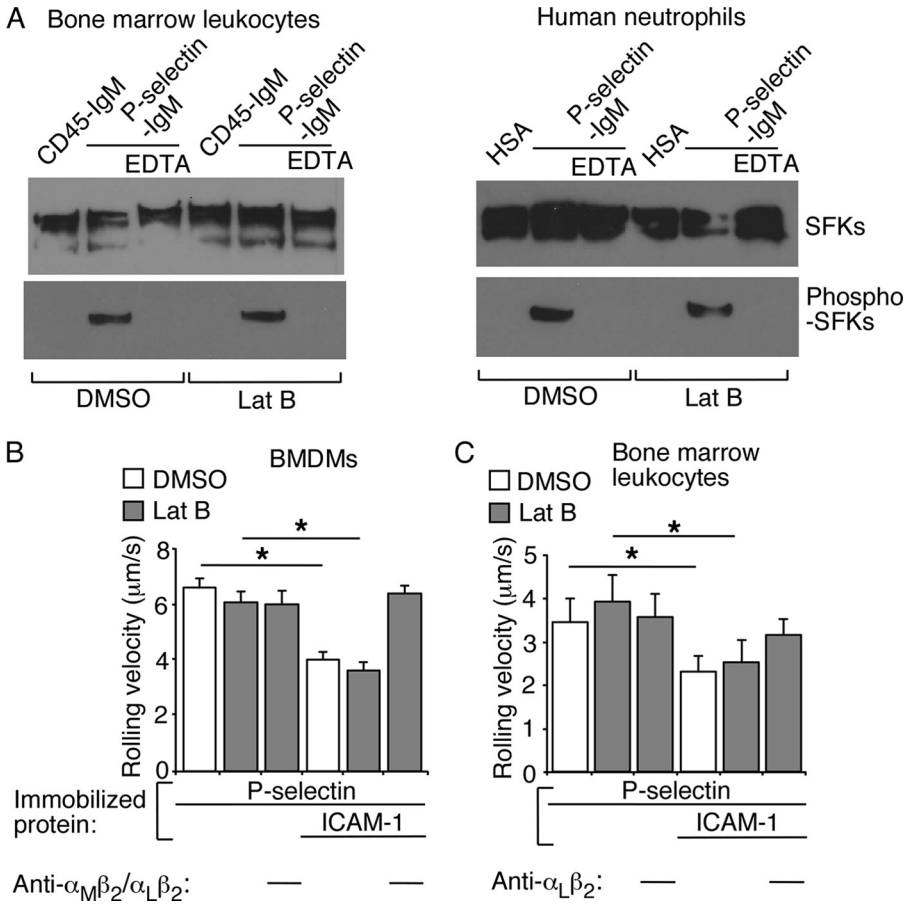

FIGURE 6. **Neutrophils or BMDMs do not require an intact actin cytoskeleton to initiate signaling and induce β_2 integrin-mediated slow rolling on P-selectin and ICAM-1.** *A,* DMSO- or latrunculin B (*Lat B*)-treated human neutrophils or murine bone marrow leukocytes were rotated on immobilized P-selectin-IgM or control CD45-IgM in buffer containing Ca^{2+} or EDTA for 5 min. Lysates were probed by Western blotting with antibodies to total SFK or phospho-SFK (Y416). The data are representative of three experiments. *B,* velocities of DMSO- or latrunculin B (*Lat B*)-treated BMDMs rolling on P-selectin with or without coimmobilized ICAM-1 in the presence or absence of blocking mAbs to integrins $\alpha_M\beta_2$ and $\alpha_L\beta_2$. *C,* velocities of DMSO- or latrunculin B (*Lat B*)-treated bone marrow leukocytes rolling on P-selectin with or without coimmobilized ICAM-1 in the presence or absence of blocking mAb to integrin $\alpha_L\beta_2$. The wall shear stress in *B* and *C* was 1 dyn/cm^2. *, $p < 0.01$. The data represent the mean ± S.E. from at least three experiments.

ther murine BMDMs nor neutrophils require an intact actin cytoskeleton to roll on P-selectin or to activate β_2 integrins to slow rolling on ICAM-1.

Depolymerizing Actin Filaments in Suspended Neutrophils Does Not Prevent β_2 Integrin Extension by Soluble P-selectin or Chemokine but Impairs Hybrid Domain Swing Out by Soluble Chemokine—The mAb KIM127 binds to an epitope near the genu (knee) in the human β_2 subunit, which is exposed only after integrin extension (53). The mAb MEM148 reports "swing out" of the hybrid domain from the human β_2 I domain in an extended conformation often associated with high affinity for ligand (54). Soluble human P-selectin induced epitopes for KIM127 but not for MEM148 on suspended DMSO- or latrunculin B-treated human neutrophils (Fig. 7*A*). Soluble P-selectin did not alter binding of mAb IB4 to an activation-insensitive epitope on the β_2 subunit. Blocking Ca^{2+}-dependent binding of soluble P-selectin to PSGL-1 with EDTA prevented integrin extension, confirming its specificity (Fig. 7*A*). Immunofluorescence microscopy documented altered phalloidin staining in latrunculin B-treated human neutrophils (supplemental Fig. 3*C*). Latrunculin B treatment did not affect global expression of PSGL-1 (supplemental Fig. 4). Thus, ligand engagement of PSGL-1 at zero force triggers integrin extension without external force applied by bound antibody and with little or no internal force from the cytoskeleton.

Soluble chemokine IL-8 induced epitopes for both KIM127 and MEM148 on suspended human neutrophils (Fig. 7*B*). IL-8 did not alter binding of mAb IB4 to its activation-independent epitope. Treating neutrophils with latrunculin B did not affect IL-8-stimulated binding of KIM127 but significantly decreased IL-8-stimulated binding of MEM148. We observed similar effects in neutrophils treated with blebbistatin, which inhibits energy-dependent myosin II ATPase activity and reduces actomyosin tension without depolymerizing actin filaments (Fig. 7*B*) (55). Thus, soluble chemokine triggers β_2 integrin extension and hybrid-domain swing out without external force applied by bound antibody. Unlike integrin extension, hybrid domain swing out requires intact actin filaments and actomyosin tension.

Depolymerizing Actin Filaments or Decreasing Actomyosin Tension in Rolling Neutrophils Does Not Prevent P-selectin- or Chemokine-mediated Neutrophil Arrest on KIM127 but prevents Chemokine-mediated Neutrophil Arrest on MEM148 or ICAM-1—Human neutrophils rolling on P-selectin rapidly arrested on coimmobilized KIM127 but arrested on coimmobilized ICAM-1 or MEM148 only with coimmobilized IL-8

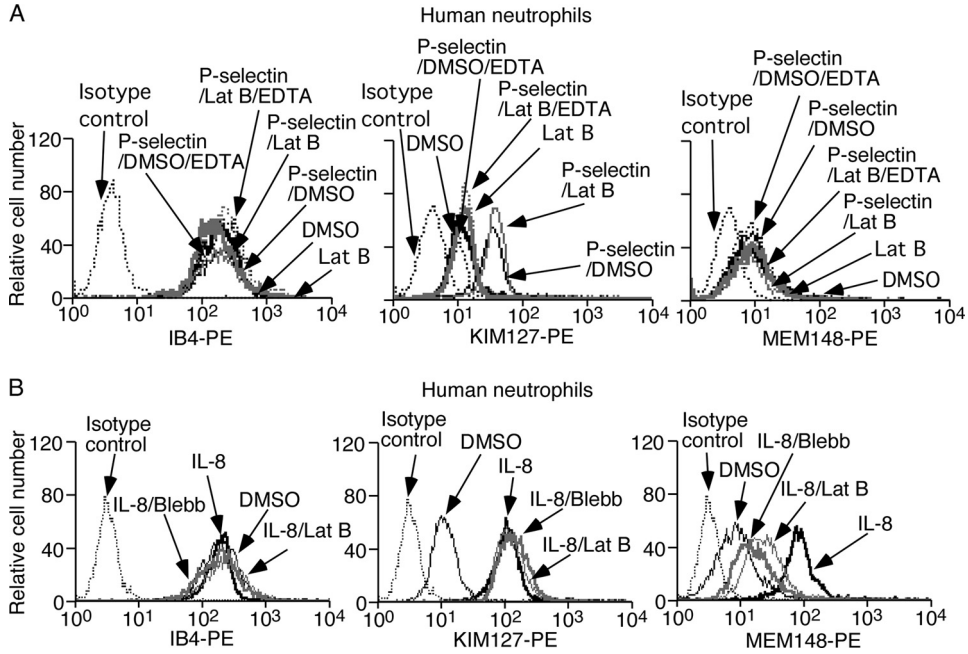

FIGURE 7. **Depolymerizing actin filaments in suspended neutrophils does not prevent β_2 integrin extension by soluble P-selectin or chemokine but impairs hybrid domain swing out by soluble chemokine.** *A,* DMSO- or latrunculin B (*Lat B*)-treated human neutrophils were incubated with platelet-derived P-selectin in buffer containing Ca^{2+} or EDTA. The cells were incubated with mAb IB4, KIM127, or MEM148 and then with PE-conjugated anti-mouse IgG and analyzed by flow cytometry. *B,* untreated human neutrophils were incubated with isotope control mAb or mAb IB4, KIM127, or MEM148 and then with PE-conjugated anti-mouse IgG. Alternatively, DMSO-, latrunculin B-, or blebbistatin (*Blebb*)-treated human neutrophils were stimulated with IL-8, incubated with mAb IB4, KIM127, or MEM148 and then with PE-conjugated anti-mouse IgG, and analyzed by flow cytometry. The data are representative of three experiments.

(Fig. 8*A*). Treatment with latrunculin B or blebbistatin did not prevent human neutrophils rolling on P-selectin from arresting on KIM127 with or without coimmobilized IL-8. Thus, immobilized P-selectin and/or chemokine triggers β_2 integrin extension without an intact actin cytoskeleton. In contrast, both treatments prevented human neutrophils rolling on P-selectin from arresting on ICAM-1 or MEM148 coimmobilized with IL-8. Furthermore, latrunculin B prevented murine neutrophils or BMDMs rolling on P-selectin from arresting on ICAM-1 coimmobilized with murine chemokine CCL2 or CXCL1, respectively (Fig. 8, *B* and *C*). Thus, neutrophils expressing chemokine-primed extended β_2 integrins require intact actin filaments and actomyosin tension to arrest on MEM148, which reports hybrid domain swing out, or ICAM-1, which requires conversion of β_2 integrins to their high affinity conformations.

DISCUSSION

Neutrophils rolling on P- or E-selectin trigger PSGL-1-mediated signals that activate integrin $\alpha_L\beta_2$ to slow rolling on ICAM-1. Our results provide insights into both upstream and downstream aspects of this process (Fig. 9). Receptor interactions with the actin cytoskeleton commonly enhance signaling (18–20, 23, 24). However, we found that PSGL-1 requires neither direct nor indirect interactions with the cytoskeleton to initiate signaling. Integrin-cytoskeleton interactions are closely linked to integrin activation (25, 31, 34). However, we found that $\alpha_L\beta_2$-dependent slow neutrophil rolling on P-selectin and ICAM-1 requires neither intact actin filaments nor actomyosin-mediated tension. The cytoskeletal independence of PSGL-1-initiated, $\alpha_L\beta_2$-mediated slow rolling contrasts sharply with the cytoskeletal dependence of chemokine-initiated, $\alpha_L\beta_2$-mediated arrest.

Because the PSGL-1 cytoplasmic domain binds to ERM proteins in solution (13, 14), it was assumed, but never verified, that ERM proteins link PSGL-1 to the actin cytoskeleton in cells. Our FRAP measurements provide the first direct evidence that the cytoplasmic domain interacts with the cytoskeleton to limit the lateral mobility of PSGL-1. Because the implicated juxtamembrane residues reportedly bind ERM proteins in solution, our data suggest that ERM proteins link the PSGL-1 tail to actin filaments. Nevertheless, the discordant effects of mutating the SRKS and MYVR residues on moesin binding in solution and PSGL-1 mobility in cells raise caution in assigning cellular defects solely to altered binding to ERM proteins. Membrane interactions influence the structures of cytoplasmic domains (56) and may limit access of the more proximal SRK residues in the PSGL-1 tail to ERM proteins. This could explain why mutating these residues markedly reduced binding in solution but did not alter PSGL-1 mobility in cells, although it did increase the mobile fraction. In contrast, the more distal MYVR residues may dominate binding to ERM proteins in cells but not in solution. Alternatively or in addition, sequences in the juxtamembrane PSGL-1 tail could bind to other adaptor proteins that interact with actin filaments. Remarkably, dimerization of PSGL-1 did not alter membrane mobility, distinguishing it from other membrane proteins that augment cytoskeleton-dependent clustering by dimerizing (23, 24).

The PSGL-1 tail mutations did not inhibit the numbers or velocities of transduced BMDMs rolling on P-selectin. Our results do not support a recent report that similar mutations in

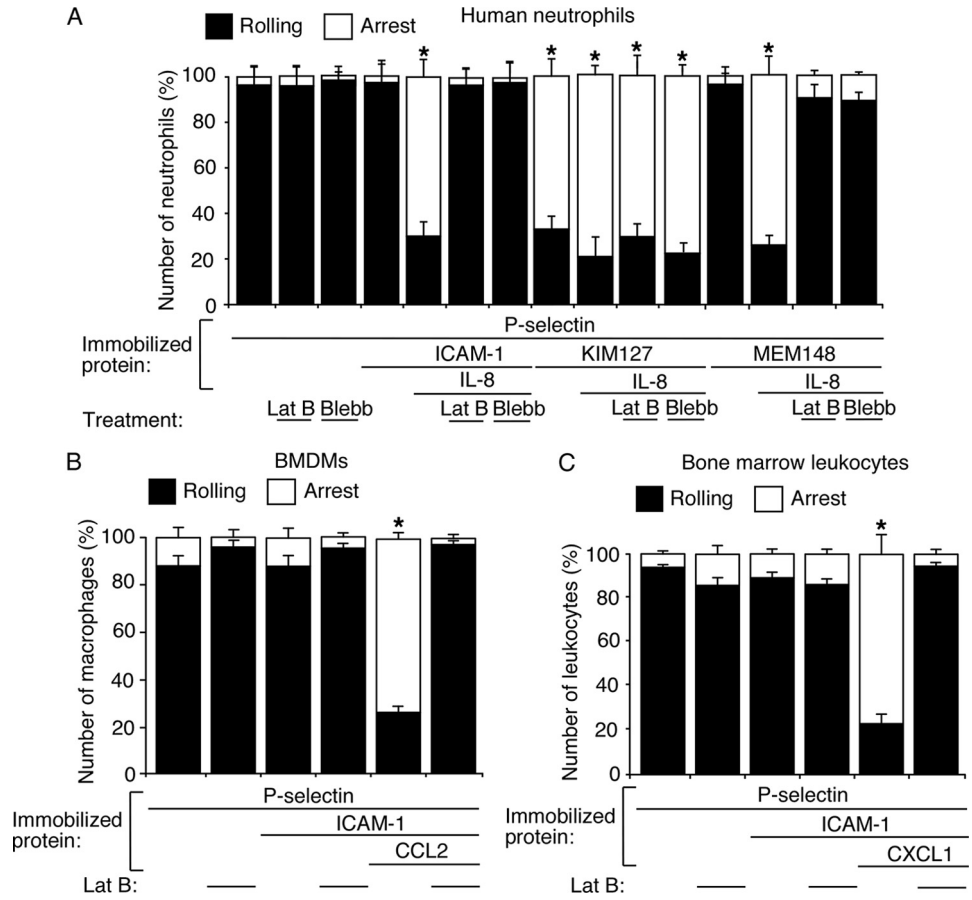

FIGURE 8. **Depolymerizing actin filaments or decreasing actomyosin tension in rolling leukocytes does not prevent chemokine-mediated arrest on KIM127 but prevents arrest on MEM148 or ICAM-1.** *A,* DMSO-, latrunculin B (*Lat B*)- or blebbistatin (*Blebb*)-treated human neutrophils were perfused over P-selectin with or without coimmobilized ICAM-1, MEM148, or chemokine IL-8. The percentage of rolling or firmly adherent (arrest) cells was plotted. *B,* DMSO- or latrunculin B-treated BMDMs were perfused over P-selectin with or without coimmobilized ICAM-1, MEM148, or chemokine CCL2. The percentage of rolling or firmly adherent (arrest) cells was plotted. *C,* DMSO- or latrunculin B-treated murine bone marrow leukocytes were perfused over P-selectin with or without coimmobilized ICAM-1, MEM148, or chemokine CXCL1. The percentage of rolling or firmly adherent (arrest) cells was plotted. The wall shear stress was 1 dyn/cm^2. The data represent the mean ± S.E. from at least three experiments. *, $p < 0.01$.

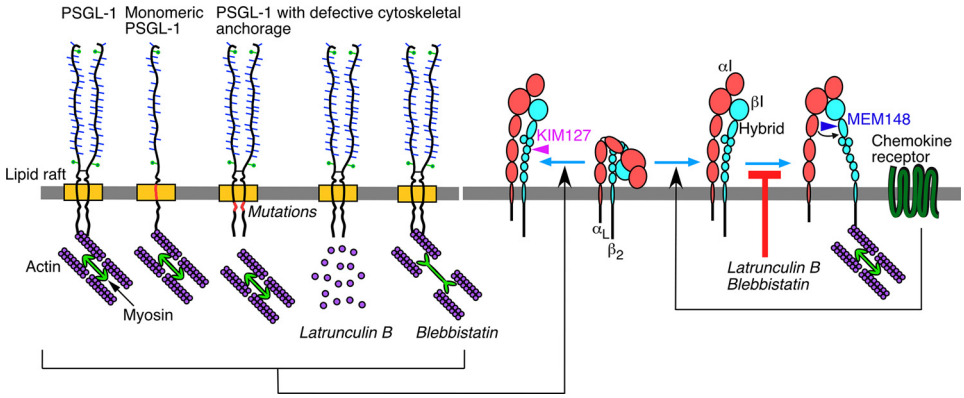

FIGURE 9. **Schematic contrasting the cytoskeletal independence of PSGL-1 or chemokine-receptor signaling that partially activates integrin $\alpha_L\beta_2$ with the cytoskeletal dependence of chemokine-receptor signaling that fully activates integrin $\alpha_L\beta_2$.** Cytoskeletal anchorage restrains the lateral mobility of dimeric or monomeric PSGL-1. Disrupting anchorage by mutating the PSGL-1 cytoplasmic domain, by depolymerizing actin filaments with latrunculin B, or by blocking actomyosin tension with blebbistatin does not prevent PSGL-1 signaling that extends $\alpha_L\beta_2$, exposes the epitope for mAb KIM127, and enables slow neutrophil rolling on ICAM-1. Neither latrunculin B nor blebbistatin prevents chemokine-receptor signaling that extends $\alpha_L\beta_2$, but both inhibitors block swing out of the hybrid domain, exposure of the epitope for mAb MEM148, and neutrophil arrest on ICAM-1. See "Discussion" for details.

the putative ERM-binding site of PSGL-1 markedly reduce the number of transfected CHO or murine 32D cells rolling on P-selectin (57), although both studies agree that cells expressing WT or mutant PSGL-1 roll with similar velocities. Our data are consistent with previous observations that deleting the entire PSGL-1 tail does not impair the numbers or velocities of neutrophils from knock-in mice or transfected CHO cells rolling on P-selectin *in vitro* (5). Indeed, despite an ~90% reduction in PSGL-1 surface density, neutrophils expressing tail-less PSGL-1 roll on P-selectin *in vivo* in greater numbers

than predicted by the *in vitro* data with transfected 32D cells (5).

We found transduced BMDMs to be a robust model for studying adhesion-dependent signaling in nontransformed myeloid cells. By the many criteria examined, BMDMs and neutrophils rolling on P-selectin employed the same signaling pathway to induce β_2 integrin-dependent slow rolling on ICAM-1. BMDMs used both $\alpha_M\beta_2$ and $\alpha_L\beta_2$ to slow rolling, in accordance with the higher expression of $\alpha_M\beta_2$ on these cells. Although neutrophils primarily use $\alpha_L\beta_2$ to slow rolling, they sometimes use $\alpha_M\beta_2$ as well (52). We expressed altered forms of PSGL-1 in BMDMs from PSGL-1-deficient mice. This strategy revealed that PSGL-1 tail mutations that disrupt cytoskeletal interactions do not impair PSGL-1-triggered slow rolling on P-selectin and ICAM-1. Our data agree with the failure of similar mutations in the human PSGL-1 tail to inhibit slow rolling of transfected 32D cells on E-selectin and ICAM-1 (57). However, this study did not address whether 32D cells, a murine myeloid cell line, express endogenous murine PSGL-1, CD44, or other E-selectin ligands that may also activate β_2 integrins to decrease rolling velocities on ICAM-1. Some 32D cells do express such ligands (58, 59). Cross-linking WT or mutated human PSGL-1 with intact primary and secondary antibodies was found to equivalently activate Syk in transfected 32D cells (57). However, no controls excluded engagement of Fc receptors by the intact antibodies. Fc receptor engagement would activate the Fc receptor γ chain, a central component of the PSGL-1 signaling cascade (8).

Disrupting direct interactions of the PSGL-1 tail with the cytoskeleton did not impair signaling. Indirect interactions with the cytoskeleton may distribute tail-less PSGL-1 to microvilli of resting neutrophils and to the uropods of chemokine-stimulated, polarized neutrophils (5). However, latrunculin B-treated neutrophils triggered $\alpha_L\beta_2$-dependent slow rolling on P-selectin and ICAM-1, demonstrating that PSGL-1 signaling does not require an intact cytoskeleton. How does PSGL-1 initiate signaling in rolling neutrophils with depolymerized actin filaments? Cholesterol-enriched membrane rafts, which concentrate many signaling proteins, may be important (60). Chelating or sequestering cholesterol blocks PSGL-1-mediated signaling (7). Actin filaments are important raft organizers (16, 17), but cholesterol-dependent raft integrity was sufficient for PSGL-1 to trigger signaling in neutrophils or BMDMs treated with latrunculin B. Although phalloidin staining confirmed that latrunculin B substantially disrupted actin filaments, remnants of the membrane cytoskeleton might cluster rafts. Alternatively, rolling neutrophils without actin filaments may coalesce small membrane domains into larger domains through reversible PSGL-1 bonds with P-selectin. Indeed, lack of cytoskeletal restraints might favor clustering of PSGL-1. In knock-in mice, neutrophils expressing PSGL-1 lacking the entire cytoplasmic domain do not signal while rolling on P- or E-selectin (5, 7), even though tail-less PSGL-1 still associates with lipid rafts (5). Therefore, portions of the cytoplasmic domain other than the ERM-binding sequence must propagate signals without requiring direct linkage to the cytoskeleton.

Both soluble and immobilized P-selectin triggered integrin extension in human neutrophils, measured by binding of mAb KIM127, even when the cells were treated with inhibitors to depolymerize actin filaments or prevent actomyosin contraction. Therefore, PSGL-1-mediated extension of $\alpha_L\beta_2$ in suspended or rolling neutrophils does not require prior integrin attachment to an intact cytoskeleton or actomyosin contraction. Furthermore, extensive cytoskeletal anchorage of $\alpha_L\beta_2$ is not needed to withstand the axial forces applied to $\alpha_L\beta_2$-ICAM-1 bonds during rolling. The "traction" model proposes that cells activated by chemokines or other agonists prime integrins to states with intermediate affinity for ligand. Transition to the high affinity state requires an energy-dependent cytoskeleton that exerts lateral force (traction) to fully separate the α and β tails. Traction develops only if the integrin binds to immobilized ligand (34). We found that PSGL-1 signaling primes $\alpha_L\beta_2$ to an extended state that is subjected to axial forces during rolling but not to the cytoskeleton-dependent lateral forces predicted by the traction model. Single particle tracking has identified a subset of mobile, "closed" (bent rather than extended) $\alpha_L\beta_2$ molecules in the plasma membranes of resting leukocytes (61). PSGL-1 signaling might preferentially act on this subset. Neither soluble nor immobilized P-selectin induced swing out of the hybrid domain in the extended β_2 subunit, measured by binding of mAb MEM148. PSGL-1-mediated signaling may cause the talin head domain to bind to the β_2 tail, weakening interactions with the α_L tail and extending the $\alpha_L\beta_2$ ectodomain (62). The talin rod domain might not interact with actin, limiting $\alpha_L\beta_2$ tail separation and preventing hybrid domain swing out. Consistent with this possibility, overexpressing the talin head domain in transfected cells separates the α_L and β_2 tails (63) but may not fully activate $\alpha_L\beta_2$ (64). Alternatively, actin filaments bound to the β_2 integrin tail could resist energy-dependent contraction by myosin. Failure to recruit kindlins to the β_2 tail may also impair cytoskeletal interactions (62).

Immobilized, but not soluble, chemokine was reported to induce integrin $\alpha_L\beta_2$ extension in human lymphocytes (31). Depolymerizing actin filaments with cytochalasin B prevented chemokine-mediated integrin extension (31). In contrast, we found that either soluble or immobilized IL-8 triggers integrin extension and hybrid domain swing out in human neutrophils. Latrunculin B treatment did not affect integrin extension but markedly inhibited hybrid domain swing out. These data demonstrate that $\alpha_L\beta_2$, at least in neutrophils, need not anchor to the cytoskeleton to extend in response to chemokine signals. In suspended neutrophils lacking an intact actin cytoskeleton, IL-8-triggered binding of talin and kindlin may transiently induce swing out of the hybrid domains in a small number of extended $\alpha_L\beta_2$ molecules, which are stabilized by saturating concentrations of MEM148. In contrast, immobilized chemokine did not induce latrunculin B-treated neutrophils rolling on P-selectin to arrest on coimmobilized ICAM-1 or MEM148. Immobilized chemokine likely fully primes only a few integrins on rolling neutrophils. Without an intact cytoskeleton, these integrins may revert to low affinity conformations too rapidly to attach to ICAM-1 or MEM148.

Dimerization and cytoskeleton-dependent clustering of receptors commonly initiate signaling. Yet PSGL-1 required neither mechanism to signal as it engaged P-selectin despite the short force-regulated bond lifetimes of rolling neutrophils under flow (2). It will be important to unravel the novel early steps by which PSGL-1 engagement triggers signals. Neutrophils rolling on E-selectin engage PSGL-1 or CD44 to induce $\alpha_L\beta_2$-mediated slow rolling on ICAM-1 (7). Although neutrophils rolling on P- or E-selectin appear to use the same overall signaling pathway, E-selectin might rely more on oligomerization or cytoskeletal interactions of its ligands during the earliest signaling steps. The downstream consequence of selectin-mediated signaling is rapid extension of integrin $\alpha_L\beta_2$, which interacts reversibly with ICAM-1 to slow rolling velocities. That rapid extension and slow rolling occurred independently of most actin filaments has implications for how talin, kindlin, and mechanical forces regulate $\alpha_L\beta_2$ conformation and function as leukocytes roll and arrest on vascular surfaces.

Acknowledgments—We thank Cheng Zhu and Renhao Li for reading the manuscript.

REFERENCES

1. Ley, K., Laudanna, C., Cybulsky, M. I., and Nourshargh, S. (2007) Getting to the site of inflammation. The leukocyte adhesion cascade updated. *Nat. Rev. Immunol.* **7,** 678–689
2. McEver, R. P., and Zhu, C. (2010) Rolling cell adhesion. *Annu. Rev. Cell Dev. Biol.* **26,** 363–396
3. Zarbock, A., Ley, K., McEver, R. P., and Hidalgo, A. (2011) Leukocyte ligands for endothelial selectins. Specialized glycoconjugates that mediate rolling and signaling under flow. *Blood* **118,** 6743–6751
4. Zarbock, A., Lowell, C. A., and Ley, K. (2007) Spleen tyrosine kinase Syk is necessary for E-selectin-induced α(L)β(2) integrin-mediated rolling on intercellular adhesion molecule-1. *Immunity* **26,** 773–783
5. Miner, J. J., Xia, L., Yago, T., Kappelmayer, J., Liu, Z., Klopocki, A. G., Shao, B., McDaniel, J. M., Setiadi, H., Schmidtke, D. W., and McEver, R. P. (2008) Separable requirements for cytoplasmic domain of PSGL-1 in leukocyte rolling and signaling under flow. *Blood* **112,** 2035–2045
6. Jung, U., Norman, K. E., Scharffetter-Kochanek, K., Beaudet, A. L., and Ley, K. (1998) Transit time of leukocytes rolling through venules controls cytokine-induced inflammatory cell recruitment *in vivo*. *J. Clin. Invest.* **102,** 1526–1533
7. Yago, T., Shao, B., Miner, J. J., Yao, L., Klopocki, A. G., Maeda, K., Coggeshall, K. M., and McEver, R. P. (2010) E-selectin engages PSGL-1 and CD44 through a common signaling pathway to induce integrin αLβ2-mediated slow leukocyte rolling. *Blood* **116,** 485–494
8. Zarbock, A., Abram, C. L., Hundt, M., Altman, A., Lowell, C. A., and Ley, K. (2008) PSGL-1 engagement by E-selectin signals through Src kinase Fgr and ITAM adapters DAP12 and FcRγ to induce slow leukocyte rolling. *J. Exp. Med.* **205,** 2339–2347
9. Mueller, H., Stadtmann, A., Van Aken, H., Hirsch, E., Wang, D., Ley, K., and Zarbock, A. (2010) Tyrosine kinase Btk regulates E-selectin-mediated integrin activation and neutrophil recruitment by controlling phospholipase C (PLC) γ2 and PI3Kγ pathways. *Blood* **115,** 3118–3127
10. Stadtmann, A., Brinkhaus, L., Mueller, H., Rossaint, J., Bolomini-Vittori, M., Bergmeier, W., Van Aken, H., Wagner, D. D., Laudanna, C., Ley, K., and Zarbock, A. (2011) Rap1a activation by CalDAG-GEFI and p38 MAPK is involved in E-selectin-dependent slow leukocyte rolling. *Eur. J. Immunol.* **41,** 2074–2085
11. Kuwano, Y., Spelten, O., Zhang, H., Ley, K., and Zarbock, A. (2010) Rolling on E- or P-selectin induces the extended but not high affinity conformation of LFA-1 in neutrophils. *Blood* **116,** 617–624
12. Del Conde, I., Shrimpton, C. N., Thiagarajan, P., and López, J. A. (2005) Tissue factor-bearing microvesicles arise from lipid rafts and fuse with activated platelets to initiate coagulation. *Blood* **106,** 1604–1611
13. Serrador, J. M., Urzainqui, A., Alonso-Lebrero, J. L., Cabrero, J. R., Montoya, M. C., Vicente-Manzanares, M., Yáñez-Mó, M., and Sánchez-Madrid, F. (2002) A juxtamembrane amino acid sequence of P-selectin glycoprotein ligand-1 is involved in moesin binding and ezrin/radixin/moesin-directed targeting at the trailing edge of migrating lymphocytes. *Eur. J. Immunol.* **32,** 1560–1566
14. Snapp, K. R., Heitzig, C. E., and Kansas, G. S. (2002) Attachment of the PSGL-1 cytoplasmic domain to the actin cytoskeleton is essential for leukocyte rolling on P-selectin. *Blood* **99,** 4494–4502
15. Neisch, A. L., and Fehon, R. G. (2011) Ezrin, Radixin, and Moesin. Key regulators of membrane-cortex interactions and signaling. *Curr. Opin. Cell Biol.* **23,** 377–382
16. Chichili, G. R., and Rodgers, W. (2007) Clustering of membrane raft proteins by the actin cytoskeleton. *J. Biol. Chem.* **282,** 36682–36691
17. Goswami, D., Gowrishankar, K., Bilgrami, S., Ghosh, S., Raghupathy, R., Chadda, R., Vishwakarma, R., Rao, M., and Mayor, S. (2008) Nanoclusters of GPI-anchored proteins are formed by cortical actin-driven activity. *Cell* **135,** 1085–1097
18. Lillemeier, B. F., Pfeiffer, J. R., Surviladze, Z., Wilson, B. S., and Davis, M. M. (2006) Plasma membrane-associated proteins are clustered into islands attached to the cytoskeleton. *Proc. Natl. Acad. Sci. U.S.A.* **103,** 18992–18997
19. Lillemeier, B. F., Mörtelmaier, M. A., Forstner, M. B., Huppa, J. B., Groves, J. T., and Davis, M. M. (2010) TCR and Lat are expressed on separate protein islands on T cell membranes and concatenate during activation. *Nat. Immunol.* **11,** 90–96
20. Jaqaman, K., Kuwata, H., Touret, N., Collins, R., Trimble, W. S., Danuser, G., and Grinstein, S. (2011) Cytoskeletal control of CD36 diffusion promotes its receptor and signaling function. *Cell* **146,** 593–606
21. Epperson, T. K., Patel, K. D., McEver, R. P., and Cummings, R. D. (2000) Noncovalent association of P-selectin glycoprotein ligand-1 and minimal determinants for binding to P-selectin. *J. Biol. Chem.* **275,** 7839–7853
22. Miner, J. J., Shao, B., Wang, Y., Chichili, G. R., Liu, Z., Klopocki, A. G., Yago, T., McDaniel, J. M., Rodgers, W., Xia, L., and McEver, R. P. (2011) Cytoplasmic domain of P-selectin glycoprotein ligand-1 facilitates dimerization and export from the endoplasmic reticulum. *J. Biol. Chem.* **286,** 9577–9586
23. Sigalov, A. B. (2008) Signaling chain homo-oligomerization (SCHOOL) model. *Adv. Exp. Med. Biol.* **640,** 121–163
24. Cooper, J. A., and Qian, H. (2008) A mechanism for SRC kinase-dependent signaling by noncatalytic receptors. *Biochemistry* **47,** 5681–5688
25. Kim, C., Ye, F., and Ginsberg, M. H. (2011) Regulation of integrin activation. *Annu. Rev. Cell Dev. Biol.* **27,** 321–345
26. Ye, F., Hu, G., Taylor, D., Ratnikov, B., Bobkov, A. A., McLean, M. A., Sligar, S. G., Taylor, K. A., and Ginsberg, M. H. (2010) Recreation of the terminal events in physiological integrin activation. *J. Cell Biol.* **188,** 157–173
27. Astrof, N. S., Salas, A., Shimaoka, M., Chen, J., and Springer, T. A. (2006) Importance of force linkage in mechanochemistry of adhesion receptors. *Biochemistry* **45,** 15020–15028
28. Woolf, E., Grigorova, I., Sagiv, A., Grabovsky, V., Feigelson, S. W., Shulman, Z., Hartmann, T., Sixt, M., Cyster, J. G., and Alon, R. (2007) Lymph node chemokines promote sustained T lymphocyte motility without triggering stable integrin adhesiveness in the absence of shear forces. *Nat. Immunol.* **8,** 1076–1085
29. Kong, F., García, A. J., Mould, A. P., Humphries, M. J., and Zhu, C. (2009) Demonstration of catch bonds between an integrin and its ligand. *J. Cell Biol.* **185,** 1275–1284
30. Chen, W., Lou, J., and Zhu, C. (2010) Forcing switch from short- to intermediate- and long-lived states of the αA domain generates LFA-1/ICAM-1 catch bonds. *J. Biol. Chem.* **285,** 35967–35978
31. Shamri, R., Grabovsky, V., Gauguet, J. M., Feigelson, S., Manevich, E., Kolanus, W., Robinson, M. K., Staunton, D. E., von Andrian, U. H., and Alon, R. (2005) Lymphocyte arrest requires instantaneous induction of an extended LFA-1 conformation mediated by endothelium-bound chemokines. *Nat. Immunol.* **6,** 497–506

32. Alon, R., and Dustin, M. L. (2007) Force as a facilitator of integrin conformational changes during leukocyte arrest on blood vessels and antigen-presenting cells. *Immunity* **26,** 17–27
33. Schürpf, T., and Springer, T. A. (2011) Regulation of integrin affinity on cell surfaces. *EMBO J.* **30,** 4712–4727
34. Zhu, J., Luo, B. H., Xiao, T., Zhang, C., Nishida, N., and Springer, T. A. (2008) Structure of a complete integrin ectodomain in a physiological resting state and activation and deactivation by applied forces. *Mol. Cell* **32,** 849–861
35. McEver, R. P., and Zhu, C. (2007) A catch to integrin activation. *Nat. Immunol.* **8,** 1035–1037
36. Moore, K. L., Patel, K. D., Bruehl, R. E., Li, F., Johnson, D. A., Lichenstein, H. S., Cummings, R. D., Bainton, D. F., and McEver, R. P. (1995) P-selectin glycoprotein ligand-1 mediates rolling of human neutrophils on P-selectin. *J. Cell Biol.* **128,** 661–671
37. Xia, L., Sperandio, M., Yago, T., McDaniel, J. M., Cummings, R. D., Pearson-White, S., Ley, K., and McEver, R. P. (2002) P-selectin glycoprotein ligand-1-deficient mice have impaired leukocyte tethering to E-selectin under flow. *J. Clin. Invest.* **109,** 939–950
38. Gimferrer, I., Hu, T., Simmons, A., Wang, C., Souabni, A., Busslinger, M., Bender, T. P., Hernandez-Hoyos, G., and Alberola-Ila, J. (2011) Regulation of GATA-3 expression during CD4 lineage differentiation. *J. Immunol.* **186,** 3892–3898
39. Lo, W., Rodgers, W., and Hughes, T. (1998) Making genes green. Creating green fluorescent protein (GFP) fusions with blunt-end PCR products. *BioTechniques* **25,** 94–96
40. Vedham, V., Phee, H., and Coggeshall, K. M. (2005) Vav activation and function as a rac guanine nucleotide exchange factor in macrophage colony-stimulating factor-induced macrophage chemotaxis. *Mol. Cell. Biol.* **25,** 4211–4220
41. Sharma, P., Varma, R., Sarasij, R. C., Ira, Gousset, K., Krishnamoorthy, G., Rao, M., and Mayor, S. (2004) Nanoscale organization of multiple GPI-anchored proteins in living cell membranes. *Cell* **116,** 577–589
42. Xia, L., Ramachandran, V., McDaniel, J. M., Nguyen, K. N., Cummings, R. D., and McEver, R. P. (2003) N-terminal residues in murine P-selectin glycoprotein ligand-1 required for binding to murine P-selectin. *Blood* **101,** 552–559
43. Rodgers, W., Jordan, S. J., and Capra, J. D. (2002) Transient association of Ku with nuclear substrates characterized using fluorescence photobleaching. *J. Immunol.* **168,** 2348–2355
44. Ushiyama, S., Laue, T. M., Moore, K. L., Erickson, H. P., and McEver, R. P. (1993) Structural and functional characterization of monomeric soluble P-selectin and comparison with membrane P-selectin. *J. Biol. Chem.* **268,** 15229–15237
45. Sarvepalli, D. P., Schmidtke, D. W., and Nollert, M. U. (2009) Design considerations for a microfluidic device to quantify the platelet adhesion to collagen at physiological shear rates. *Ann. Biomed. Eng.* **37,** 1331–1341
46. Nalayanda, D. D., Kalukanimuttam, M., and Schmidtke, D. W. (2007) Micropatterned surfaces for controlling cell adhesion and rolling under flow. *Biomed. Microdevices* **9,** 207–214
47. Yonemura, S., Hirao, M., Doi, Y., Takahashi, N., Kondo, T., and Tsukita, S. (1998) Ezrin/radixin/moesin (ERM) proteins bind to a positively charged amino acid cluster in the juxta-membrane cytoplasmic domain of CD44, CD43, and ICAM-2. *J. Cell Biol.* **140,** 885–895
48. Takai, Y., Kitano, K., Terawaki, S., Maesaki, R., and Hakoshima, T. (2007) Structural basis of PSGL-1 binding to ERM proteins. *Genes Cells* **12,** 1329–1338
49. Coué, M., Brenner, S. L., Spector, I., and Korn, E. D. (1987) Inhibition of actin polymerization by latrunculin A. *FEBS Lett.* **213,** 316–318
50. Rotblat, B., Prior, I. A., Muncke, C., Parton, R. G., Kloog, Y., Henis, Y. I., and Hancock, J. F. (2004) Three separable domains regulate GTP-dependent association of H-ras with the plasma membrane. *Mol. Cell. Biol.* **24,** 6799–6810
51. Dorsch, S., Klotz, K. N., Engelhardt, S., Lohse, M. J., and Bünemann, M. (2009) Analysis of receptor oligomerization by FRAP microscopy. *Nat. Methods* **6,** 225–230
52. Dunne, J. L., Ballantyne, C. M., Beaudet, A. L., and Ley, K. (2002) Control of leukocyte rolling velocity in TNF-α-induced inflammation by LFA-1 and Mac-1. *Blood* **99,** 336–341
53. Luo, B. H., Carman, C. V., and Springer, T. A. (2007) Structural basis of integrin regulation and signaling. *Annu Rev. Immunol.* **25,** 619–647
54. Tang, R. H., Tng, E., Law, S. K., and Tan, S. M. (2005) Epitope mapping of monoclonal antibody to integrin αLβ2 hybrid domain suggests different requirements of affinity states for intercellular adhesion molecules (ICAM)-1 and ICAM-3 binding. *J. Biol. Chem.* **280,** 29208–29216
55. Kovács, M., Tóth, J., Hetényi, C., Málnási-Csizmadia, A., and Sellers, J. R. (2004) Mechanism of blebbistatin inhibition of myosin II. *J. Biol. Chem.* **279,** 35557–35563
56. Deng, W., Srinivasan, S., Zheng, X., Putkey, J. A., and Li, R. (2011) Interaction of calmodulin with L-selectin at the membrane interface. Implication on the regulation of L-selectin shedding. *J. Mol. Biol.* **411,** 220–233
57. Spertini, C., Baïsse, B., and Spertini, O. (2012) Ezrin-radixin-moesin-binding sequence of PSGL-1 glycoprotein regulates leukocyte rolling on selectins and activation of extracellular signal-regulated kinases. *J. Biol. Chem.* **287,** 10693–10702
58. Lenter, M., Levinovitz, A., Isenmann, S., and Vestweber, D. (1994) Monospecific and common glycoprotein ligands for E- and P-selectin on myeloid cells. *J. Cell Biol.* **125,** 471–481
59. Katayama, Y., Hidalgo, A., Chang, J., Peired, A., and Frenette, P. S. (2005) CD44 is a physiological E-selectin ligand on neutrophils. *J. Exp. Med.* **201,** 1183–1189
60. Simons, K., and Gerl, M. J. (2010) Revitalizing membrane rafts. New tools and insights. *Nat. Rev. Mol. Cell Biol.* **11,** 688–699
61. Cairo, C. W., Mirchev, R., and Golan, D. E. (2006) Cytoskeletal regulation couples LFA-1 conformational changes to receptor lateral mobility and clustering. *Immunity* **25,** 297–308
62. Lefort, C. T., Rossaint, J., Moser, M., Petrich, B. G., Zarbock, A., Monkley, S. J., Critchley, D. R., Ginsberg, M. H., Fassler, R., and Ley, K. (2012) Distinct roles for talin-1 and kindlin-3 in LFA-1 extension and affinity regulation. *Blood,* **119,** 4275–4282
63. Kim, M., Carman, C. V., and Springer, T. A. (2003) Bidirectional transmembrane signaling by cytoplasmic domain separation in integrins. *Science* **301,** 1720–1725
64. Li, Y. F., Tang, R. H., Puan, K. J., Law, S. K., and Tan, S. M. (2007) The cytosolic protein talin induces an intermediate affinity integrin αLβ2. *J. Biol. Chem.* **282,** 24310–24319